Conservative Explicit Unrestricted-Time-Step Multidimensional Constancy-Preserving Advection Schemes

B. P. LEONARD

Center for Computational Mechanics, The University of Akron, Akron, Ohio

A. P. LOCK AND M. K. MACVEAN

The Meteorological Office, Atmospheric Processes Research Division, Bracknell, Berkshire, England

(Manuscript received 18 October 1995, in final form 28 May 1996)

ABSTRACT

The multidimensional advection schemes described in this study are based on a strictly conservative flux-based control-volume formulation. They use an explicit forward-in-time update over a single time step, but there are no "stability" restrictions on the time step. Genuinely multidimensional forward-in-time advection schemes require an estimate of transverse contributions to each face-normal flux for stability. Traditional operator-splitting techniques based on sequential one-dimensional updates introduce such transverse cross-coupling automatically; however, they have serious shortcomings. For example, conservative-form operator splitting is indeed globally conservative but introduces a serious "splitting error"; in particular, a constant is not preserved in general solenoidal velocity fields. By contrast, advective-form operator splitting is constancy preserving but not conservative. However, by using advective-form estimates for the transverse contributions together with an overall conservative-form update, strictly conservative constancy-preserving schemes can be constructed. The new methods have the unrestricted-time-step advantages of semi-Lagrangian schemes, but with the important additional attribute of strict conservation due to their flux-based formulation. Shape-preserving techniques developed for small time steps can be incorporated. For large time steps, results are not strictly shape preserving but, in practice, deviations appear to be very slight so that overall behavior is essentially shape preserving. Since only one-dimensional flux calculations are required at each step of the computation, the algorithms described here should be highly compatible with existing advection codes based on conventional operator-splitting methods. Capabilities of the new schemes are demonstrated using the well-known scalar advection test problem devised by Smolarkiewicz.

1. Introduction

Consider the pure advection equation for a volume-specific scalar ϕ in a constant-density fluid with a known velocity field $\mathbf{v}$,

$$\frac{\partial \phi}{\partial t} + \nabla \cdot (\mathbf{v}\phi) = 0. \qquad (1)$$

A practical scheme will need to successfully handle diffusion, source terms, nonconstant densities, and unsteady velocities; but simulation of Eq. (1), even in the seemingly simple case of steady two-dimensional divergence-free flow using a uniform square computational grid, still represents one of the main bottlenecks to progress.

An advection scheme should possess a number of useful attributes. We prefer to work with an *explicit forward-in-time update* over a single time step; this is achieved in principle by averaging Eq. (1) in time over Δt. In many cases, explicit schemes can be constructed *without restrictions on the time step,* other than those dictated by accuracy considerations; the so-called CFL condition is, in fact, irrelevant (Leonard 1994; Leonard et al. 1995a). A *finite-volume flux-based formulation* is obtained in principle by integrating Eq. (1) over a control volume (in addition to averaging over Δt); this means that the updated quantity is the (control-volume) *cell average* of ϕ. In this case, *conservation is guaranteed* by face flux uniqueness—the flux leaving a given control-volume cell through a particular face is then identical to the flux entering the adjacent cell through that face. In a solenoidal (although perhaps highly deformational) velocity field, an initially homogeneous scalar governed by Eq. (1) should remain identically equal to the initial constant value everywhere; we call this the *constancy condition.* [Schemes based on conservative-form operator splitting violate this condition; the resulting "splitting error" can be quite substantial, leading to a phenomenon we call

Corresponding author address: Dr. B. P. Leonard, Department of Mechanical Engineering, Center for Computational Mechanics, The University of Akron, Akron, OH 44325-3903.

"lumpiness."] In an explicit forward-in-time multidimensional update for unsteady flow, one cannot merely add one-dimensional contributions to the net flux in each face-normal direction simultaneously; the resulting scheme would be unstable in general—a genuinely multidimensional forward-in-time algorithm requires estimates of *transverse* contributions to each face flux as well. It is also important to be able to structure the algorithm to include high formal accuracy; although the cost of a higher-order method is greater (per space–time grid point), the concomitant increase in accuracy more than offsets the larger cost, thereby greatly enhancing *computational efficiency.* We recommend formal *third*-order accuracy as a minimum, and prefer to work with nominally fifth- and higher- (odd) order schemes in some cases. Finally, an advection scheme should be *shape preserving;* it should not accentuate local extrema (although it should not unphysically "clip" extrema either). Unsophisticated advection schemes tend to produce unphysical undershoots (overshoots) and numerical oscillations in regions involving sudden changes in gradient of the advected variable; avoidance of this anomalous behavior is related to questions of shape preservation in the *subcell interpolation* used in calculating advective fluxes.

An advection algorithm possessing all of the attributes mentioned would, indeed, be highly attractive. Unfortunately, it seems difficult to satisfy all criteria simultaneously. Good progress has been made with explicit *one-dimensional* advection schemes, with extension to flux-based conservative unrestricted-time-step formulations occurring quite recently. One example is our NIRVANA strategy (Leonard et al. 1995a); see also Roache (1992) and Leonard (1994). Many multidimensional schemes are based on unsophisticated operator-splitting methods using successive one-dimensional updates in each coordinate direction sequentially. If *conservative-form* (sometimes called flux form) one-dimensional operators are used for each direction, the overall multidimensional update is indeed globally conservative but does not preserve constancy. In a general case, quite large splitting errors may be introduced and in some cases (e.g., steady deformational advection fields), this can lead to an unstable secular growth of local errors. Shape preservation also suffers for related reasons. By contrast, entirely *advective-form* operator splitting (described in detail below) preserves constancy automatically, and one-dimensional shape-preserving operators maintain shape preservation in multidimensions as well—even for arbitrarily large Δt. Unfortunately this technique is not conservative.

In recent years, explicit semi-Lagrangian methods (see the review by Staniforth and Côté 1991) have had a rapid rise in popularity due primarily to their lack of time-step restrictions (other than those related to accuracy considerations). By using appropriate interpolation for the so-called departure point, these techniques can be highly accurate and shape preserving. However, once again, semi-Lagrangian methods are not inherently conservative.

A number of conservative explicit genuinely multidimensional forward-in-time advection schemes have been developed in the past (Dukowicz and Ramshaw 1979; Smolarkiewicz 1984). In recent years, multidimensional advection schemes have been extended to higher-order accuracy (Ekebjærg and Justesen 1991; Rasch 1994; Hólm 1995), some with consistently formulated higher-order diffusion terms as well, such as our flux-integral method (Leonard et al. 1995b). These particular schemes all have time-step restrictions equivalent to requiring component Courant numbers to be generally less than $O(1)$, plus additional diffusive time-step constraints. They can be rendered shape preserving by using multidimensional flux limiters (Leonard et al. 1993; Hólm 1995; Thuburn 1996).

We recently combined elements of our flux-integral method with NIRVANA concepts resulting in the ENIGMATIC code (Leonard et al. 1995c), a conservative explicit unrestricted-time-step genuinely multidimensional constancy-preserving scheme. It is not possible to develop a *strictly* shape-preserving version of ENIGMATIC for large Δt and general deformational velocity fields; however, in most cases of practical interest, lack of shape preservation appears to be minimal. We call this behavior *essentially shape preserving* (ESP).

The advection schemes described in the present paper have the same general properties as ENIGMATIC. They are, however, somewhat more straightforward conceptually, being based on principles closely related to operator splitting. In fact, the resulting advection schemes should be highly compatible with codes currently using conventional operator-splitting techniques.

While the present manuscript was under review, the very recent paper by Lin and Rood (1996) was brought to our attention. The general principles of the method described in that paper are essentially the same as some of those outlined here: using combinations of advective-form and conservative-form operator splitting. Differences occur in the details of implementation, especially in the one-dimensional flux-difference calculations and the treatment of transverse velocity components.

The following section outlines the general principles of constructing finite-volume formulations. Section 3 summarizes operator-splitting techniques, and section 4 introduces an operator notation for flux-difference splitting. The construction of schemes that are both conservative and constancy preserving is outlined in section 5, with extension to three dimensions in section 6. Questions of shape preservation are considered in section 7 and computational efficiency is discussed in section 8. Conclusions and suggestions for further development are given in section 9.

2. Explicit update equation

The basic forward-in-time explicit update algorithm for cell-average values is obtained by averaging Eq. (1) over a single time step Δt and integrating over a finite-volume cell of volume V. Using Gauss's divergence theorem, this results in

$$V\left(\frac{\bar{\phi}^+ - \bar{\phi}}{\Delta t}\right) = -\sum_f A_f \langle \widetilde{v_f \phi_f} \rangle, \tag{2}$$

where bars signify cell-average values, the plus-sign superscript indicates the updated value, A_f is a finite-volume face area, v_f represents the outward normal component of advecting velocity, ϕ_f is an instantaneous face value, the angle brackets represent surface averages over individual faces, and the tilde refers to the time average over Δt. This equation is exact.

A fundamental approximation usually assumes that the instantaneous advecting velocity component and advected scalar are uncorrelated with respect to the averaging operations; that is,

$$\langle \widetilde{v_f \phi_f} \rangle \approx \langle \tilde{v}_f \rangle \langle \tilde{\phi}_f \rangle. \tag{3}$$

This is clearly questionable when ϕ is a strong function of velocity (e.g., advection of momentum, vorticity, etc.); however, it appears to be a less serious approximation in general compared to others involved in the final form of the overall algorithm.

The primary task (and this is common to many explicit advection scheme constructions) is to make an estimate of the "effective" face value of ϕ, given a knowledge of all cell-average values up to the current time level; that is,

$$\phi_f^{\text{eff}} \approx \langle \widetilde{\phi_f} \rangle. \tag{4}$$

Once this is achieved, the explicit update equation becomes

$$\bar{\phi}^+ = \bar{\phi} + \sum_{\text{in}} c_f^{\text{in}} \phi_f^{\text{eff}} - \sum_{\text{out}} c_f^{\text{out}} \phi_f^{\text{eff}} \tag{5}$$

introducing inflow and outflow Courant number normal components. The steady, constant-density continuity equation (discrete solenoidal condition) then becomes, for each cell,

$$\sum_{\text{in}} c_f^{\text{in}} - \sum_{\text{out}} c_f^{\text{out}} = 0. \tag{6}$$

To construct a conservative advection algorithm for $\bar{\phi}$, it is important that both the advect*ing* normal velocity components and the advect*ed* effective scalar face values be *unique* to the particular face in question (independent of which control-volume cell they are related to). This is usually the case for the effective face values. The fundamental difference between "conservative-form" and "advective-form" formulations is in the treatment of the velocities (Smolarkiewicz and Rasch 1991). In the conservative form, the velocity components are indeed unique to each face, as described above. In the advective form, the velocities used are unique to particular control-volume cells rather than to individual faces. In general, for an advective-form algorithm, an inflow velocity on a particular face relative to the adjacent downstream cell will *not* be the same as the outflow velocity on that face relative to the adjacent upstream cell. Thus, fluxes are nonunique and conservation is destroyed.

Consider the simplest possible case of steady two-dimensional solenoidal flow, using a uniform square grid of mesh width h. The explicit update in *conservative form* is then

$$\bar{\phi}^+ = \bar{\phi} + c_{xw}\phi_w^{\text{eff}} - c_{xe}\phi_e^{\text{eff}} + c_{ys}\phi_s^{\text{eff}} - c_{yn}\phi_n^{\text{eff}}, \tag{7}$$

using standard compass-point notation and defining individual face Courant number normal components as $c_{xw} = u_w \Delta t/h$, etc. The corresponding *advective-form* update can be written

$$\bar{\phi}^+ = \bar{\phi} + c_x^{\text{cell}}(\phi_w^{\text{eff}} - \phi_e^{\text{eff}}) + c_y^{\text{cell}}(\phi_s^{\text{eff}} - \phi_n^{\text{eff}}), \tag{8}$$

where the notation implies that the velocity components are unique to particular cells (although not necessarily cell centered).

If $\bar{\phi}$ is initially homogeneous ($\equiv \bar{\phi}_0$, say), any "reasonable" advection scheme would be expected to estimate all effective face values as being identically equal to $\bar{\phi}_0$ as well. Since the continuity equation in this case is

$$c_{xw} - c_{xe} + c_{ys} - c_{yn} = 0, \tag{9}$$

this means that the conservative-form multidimensional update, Eq. (7), automatically preserves constancy, as it should. The advective form, Eq. (8), does too—simply because the individual component face-value contributions cancel. In a more general case involving variable $\bar{\phi}$, the advective form is not conservative because of nonuniqueness of face fluxes.

3. Operator-splitting schemes

To construct a specific algorithm, one might try to estimate the effective face values in Eq. (7), say, with some reliable one-dimensional formulas (based on the current $\bar{\phi}$ values) in each coordinate direction; that is, a simple-minded update of this type might be written

$$\bar{\phi}^+_{\text{SM}} = \bar{\phi} + c_{xw}\phi_w^{\text{1D}}(\bar{\phi}) - c_{xe}\phi_e^{\text{1D}}(\bar{\phi}) + c_{ys}\phi_s^{\text{1D}}(\bar{\phi}) - c_{yn}\phi_n^{\text{1D}}(\bar{\phi}). \tag{10}$$

However, except for the first-order (donor-cell) method, this equation is unstable—apart from obvious degenerate cases of uniform (one-dimensional) advection along a particular coordinate direction. This was first pointed out by Leith (1965) in relation to second-

order methods but it is true for all methods higher than first order.

A von Neumann stability analysis suggests why this instability occurs. Using the standard notation

$$\theta_x = k_x h, \quad \theta_y = k_y h, \tag{11}$$

for nondimensional wavenumbers, the two-dimensional complex amplitude ratio G for the exact advection equation is (Leonard et al. 1993)

$$G_{\text{exact}} = \exp[-\iota(\mathfrak{c}\cdot\boldsymbol{\theta})] = \exp[-\iota(c_x\theta_x + c_y\theta_y)], \tag{12}$$

where $\iota = \sqrt{-1}$. In expanded form, this is

$$G_{\text{exact}} = 1 - \frac{1}{2}(c_x\theta_x + c_y\theta_y)^2 + \cdots - \iota[(c_x\theta_x + c_y\theta_y) - \frac{1}{6}(c_x\theta_x + c_y\theta_y)^3 + \cdots]. \tag{13}$$

For the first-order donor-cell method,

$$G_{1\text{st}}^{\text{SM}} = 1 - \iota(c_x\theta_x + c_y\theta_y) + O(\theta_x^2) + O(\theta_y^2), \tag{14}$$

thus matching Eq. (13) through *all* first-order terms. Using second-order one-dimensional face values such as the Lax–Wendroff (1960) or Leith (1965) method, for example, leads to

$$G_{2\text{nd}}^{\text{SM}} = 1 - \frac{1}{2}(c_x^2\theta_x^2 + c_y^2\theta_y^2) + O(\theta_x^4) + O(\theta_y^4) - \iota[(c_x\theta_x + c_y\theta_y) + O(\theta_x^3) + O(\theta_y^3)]. \tag{15}$$

This is missing the critical second-order cross term, $c_x\theta_x c_y\theta_y$. The lack of this term is responsible for the basic instability of higher-order schemes using coordinate-wise one-dimensional fluxes.

The cross terms appearing in Eq. (13) are of fundamental importance in constructing stable two-dimensional algorithms. Similar additional terms are necessary in three dimensions. Such cross terms can be introduced in two different ways:

(i) conventional operator splitting using *sequential* one-dimensional updates in each coordinate direction, and

(ii) building in *transverse* contributions to the estimates of the effective multidimensional face values directly.

Our flux-integral method, Leonard et al. (1995b), for example, and the related earlier methods of Dukowicz and Ramshaw (1979), Smolarkiewicz (1984), Ekebjærg and Justesen (1991), Rasch (1994), and Hólm (1995), introduce the necessary cross terms in Eq. (13) via explicit transverse contributions to the effective face values. This is also true of ENIGMATIC (Leonard et al. 1995c) for arbitrarily large Δt. Conventional operator-splitting methods are stable in the above sense (as discussed in detail below). The main problems with operator-splitting schemes are the following.

(i) If advective-form operator splitting is used at each step in the process, the overall update is constancy preserving but not conservative.

(ii) If conservative-form operator splitting is used at each step in the process, the overall update is conservative but not constancy preserving.

The objective of our current approach, outlined below, is to combine advective-form and conservative-form (unrestricted-time-step) operators in such a way as to introduce the necessary stabilizing cross terms while still maintaining both constancy and conservation. There are a number of ways that this can be achieved using combinations of one-dimensional flux-difference operators.

4. Flux-difference splitting

Conventional *advective-form* operator splitting consists of the following steps (in two dimensions). First, an intermediate one-dimensional update is formed; for example, in the x direction:

$$\bar{\phi}_{AX} = \bar{\phi} + c_x^{\text{cell}}[\phi_w^{1\text{D}}(\bar{\phi}) - \phi_e^{1\text{D}}(\bar{\phi})], \tag{16}$$

where the face values are based on one-dimensional estimates in the x direction (normal to the faces), starting with the original cell-average values as implied by the notation. The important thing to note is that the second term on the right-hand side of Eq. (16) can be written as the difference of face fluxes but with the *same* cell-based velocity component (not necessarily cell centered) used in the determination of each flux. This, of course, destroys face-flux uniqueness and, therefore, conservation; for example, the east-face flux of cell (i, j) is not necessarily the same as the west-face flux of cell $(i + 1, j)$. The subsequent update in the y direction is based on one-dimensional estimates of north and south face values, starting with the $\bar{\phi}_{AX}$ cell averages:

$$\bar{\phi}_{AXY}^{+} = \bar{\phi}_{AX} + c_y^{\text{cell}}[\phi_s^{1\text{D}}(\bar{\phi}_{AX}) - \phi_n^{1\text{D}}(\bar{\phi}_{AX})], \tag{17}$$

again using a common cell-based velocity component. Using $\bar{\phi}_{AX}$ (rather than $\bar{\phi}$) in the arguments of $\phi_s^{1\text{D}}$ and $\phi_n^{1\text{D}}$ introduces the stabilizing cross terms. The overall update is thus *equivalent* to, in this case,

$$\bar{\phi}_{AXY}^{+} = \bar{\phi} + c_x^{\text{cell}}[\phi_w^{1\text{D}}(\bar{\phi}) - \phi_e^{1\text{D}}(\bar{\phi})] + c_y^{\text{cell}}[\phi_s^{1\text{D}}(\bar{\phi}_{AX}) - \phi_n^{1\text{D}}(\bar{\phi}_{AX})]. \tag{18}$$

Note, however, that the usual way of performing operator splitting is to overwrite the intermediate update ($\bar{\phi}_{AX}$ in this case) onto the $\bar{\phi}$ array and then subsequently overwriting $\bar{\phi}_{AX}^{+}$ onto the same array, performing the calculations sequentially, as in Eqs. (16) and (17).

One could, of course, reverse the order of coordinate-direction updates (in three dimensions, there are six possible sequences). In this case, the resulting *equivalent* overall update is

$$\bar{\phi}^{+}_{AYX} = \bar{\phi} + c_x^{\text{cell}}[\phi_w^{\text{1D}}(\bar{\phi}_{AY}) - \phi_e^{\text{1D}}(\bar{\phi}_{AY})] + c_y^{\text{cell}}[\phi_s^{\text{1D}}(\bar{\phi}) - \phi_n^{\text{1D}}(\bar{\phi})] \quad (19)$$

using a definition analogous to Eq. (16) for the intermediate $\bar{\phi}_{AY}$. To reduce any potential directional bias, it is common practice to alternate the directional sequences; that is, first (x followed by y) and then (y followed by x), etc. (Strang 1968).

If $\bar{\phi}$ is initially equal to a constant, $\bar{\phi}_0$, everywhere (and assuming consistently homogeneous face values), then it is obvious from Eqs. (16) and (17) that the updated value, $\bar{\phi}^{+}_{AXY}$, remains equal to $\bar{\phi}_0$ as well, demonstrating that the (nonconservative) advective-form operator-splitting technique maintains constancy.

It is instructive to rewrite Eqs. (16) and (17) in operator form. Let $X_A(\bar{\phi})$ represent the advective-form one-dimensional flux difference in Eq. (16), then

$$\bar{\phi}_{AX} = \bar{\phi} + c_x^{\text{cell}}[\phi_w^{\text{1D}}(\bar{\phi}) - \phi_e^{\text{1D}}(\bar{\phi})] = \bar{\phi} + X_A(\bar{\phi}) = (1 + X_A)(\bar{\phi}). \quad (20)$$

Similarly, using an analogous definition for Y_A,

$$\bar{\phi}^{+}_{AXY} = \bar{\phi}_{AX} + Y_A(\bar{\phi}_{AX}) = (1 + Y_A)(\bar{\phi}_{AX}), \quad (21)$$

or, substituting Eq. (20),

$$\bar{\phi}^{+}_{AXY} = (1 + Y_A)(1 + X_A)(\bar{\phi}). \quad (22)$$

Expanding the product of operators gives

$$\bar{\phi}^{+}_{AXY} = (1 + X_A + Y_A + Y_AX_A)(\bar{\phi}). \quad (23)$$

Reversing the order gives

$$\bar{\phi}^{+}_{AYX} = (1 + X_A + Y_A + X_AY_A)(\bar{\phi}). \quad (24)$$

Under constant-coefficient conditions, these operators lead to the correct corresponding stabilizing cross-product terms in the complex amplitude ratio. As explained above, such cross terms are missing from the simple-minded update using one-dimensional fluxes (based on $\bar{\phi}$) in both directions simultaneously in a single-step update,

$$\bar{\phi}^{+}_{\text{SM}} = (1 + X_A + Y_A)(\bar{\phi}), \quad (25)$$

thus leading to instability (except for first order, as mentioned previously).

A practical flow calculation will involve nonconstant coefficients and, possibly, nonlinearities in the flux-difference operators (such as those introduced by flux limiters). In such cases, there is no simple formula for the equivalent overall update. However, the basic stabilizing "cross-product" mechanism is still active.

Now consider a *conservative-form* one-dimensional flux-difference operator, X_C, so that

$$\bar{\phi}_{CX} = \bar{\phi} + X_C(\bar{\phi}) = \bar{\phi} + c_{xw}\phi_w^{\text{1D}}(\bar{\phi}) - c_{xe}\phi_e^{\text{1D}}(\bar{\phi}), \quad (26)$$

with an analogous formula for Y_C. The only difference between this and the advective form, Eq. (16), is that here the velocity component used in each face flux calculation is unique to that face (and therefore not the same, in general, on the two faces). Conservative-form operator splitting is then equivalent, overall, to

$$\bar{\phi}^{+}_{CXY} = \bar{\phi} + X_C(\bar{\phi}) + Y_C(\bar{\phi}_{CX}), \quad (27)$$

or, expanding the product of operators,

$$\bar{\phi}^{+}_{CXY} = (1 + X_C + Y_C + Y_CX_C)(\bar{\phi}). \quad (28)$$

Reversing the directional sequence gives

$$\bar{\phi}^{+}_{CYX} = \bar{\phi} + X_C(\bar{\phi}_{CY}) + Y_C(\bar{\phi}) \quad (29)$$

or

$$\bar{\phi}^{+}_{CYX} = (1 + X_C + Y_C + X_CY_C)(\bar{\phi}). \quad (30)$$

Again, the cross terms are responsible for multidimensional stability. In this case, conservation is guaranteed (because of face flux uniqueness) but constancy is destroyed. To see this, assume that, as usual, $\bar{\phi} = \phi_w^{\text{1D}} = \phi_e^{\text{1D}} = \bar{\phi}_0$ in Eq. (26). Then

$$\bar{\phi}_{CX} = (1 + c_{xw} - c_{xe})\phi_0 \neq \phi_0, \quad (31)$$

since $c_{xw} \neq c_{xe}$, in general. In fact, $\bar{\phi}_{CX}$ varies from cell to cell, depending on local deformational behavior of the velocity field, so that the subsequent y-direction update produces a splitting error appropriately described as lumpiness. Of course, a similar splitting error is always present (for variable $\bar{\phi}$) in all calculations based on conservative-form operator splitting wherever $\bar{\phi}$ differs from zero. In general, this can lead to significant error and even a form of instability (a secular growth of error in steady velocity fields), as mentioned before.

As an example of the splitting-error lumpiness introduced by conventional alternating-direction conservative-form operator splitting, Fig. 1 shows results for the well-known test problem devised by Smolarkiewicz (1982) of advection of a scalar field, initially in the shape of a cone, by a strongly deformational velocity field. In this case, however, a constant equal to the height of the cone (which has been normalized to one unit) has been added to the initial scalar field, although in the figure we have plotted $\bar{\phi} - 1$, for convenience. In appendix A, we discuss the exact solution to this problem in terms of cell averages; this is different in significant ways from the nodal-point-value solution portrayed by Staniforth et al. (1987). The particular calculation shown in Fig. 1 used our one-dimensional unrestricted-time-step NIRVANA scheme (Leonard et al. 1995a) in conservative (but variable-velocity) form. In this case, we used an unlimited piecewise-fifth-order algorithm for calculating individual one-dimensional fluxes. For the control-volume cell size shown, $h = 0.5$ units (i.e., there are 50×50 cells per velocity cell, as explained in appendix A); the maximum component Courant number is $c_{\max} = 2.64$. The computation is over the 4×4 velocity-cell region shown in Fig. A1;

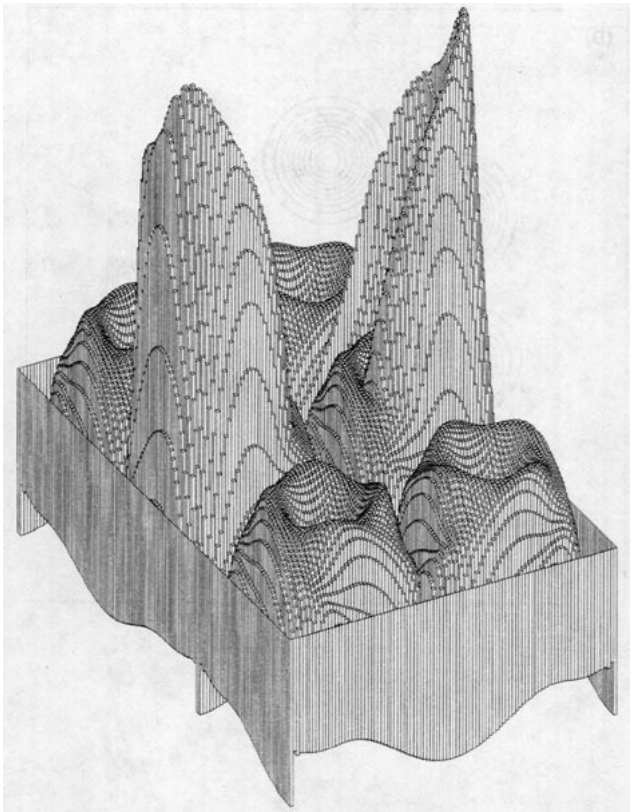

FIG. 1. Splitting-error lumpiness introduced by conventional alternating-direction conservative-form operator splitting applied to the "raised" Smolarkiewicz test problem. Plotted results show $(\bar{\phi} - 1)$ at $t = 3T/200$.

for convenience, only a 2×3 velocity-cell region is shown in Fig. 1 (and other subsequent figures showing results for this problem). Note how the main signal has been almost swamped (in comparison with the exact solution of Fig. A2) by the splitting-error lumpiness, which continues to grow, ultimately dominating the solution. If the original specifications of the Smolarkiewicz problem are used, the background lumpiness is not generated immediately, simply because the constant background field is zero. However, a corruptive splitting error of this kind is still present, in general, wherever the advected field differs from zero, for any calculation involving entirely conservative-form operator splitting.

5. Conservation plus constancy

The magnitude of the splitting error, discussed in the previous section, can be reduced (to second order in time) either through so-called Strang splitting (Strang 1968) or through corrections to the advecting velocity field, with comparable results (Hundsdorfer and Spee 1995). In this paper we take an alternative approach in order to completely eliminate splitting error lumpiness while precisely maintaining conservation by combining advective-form and conservative-form one-dimensional flux-difference operators. A number of strategies are outlined here. Specific comparisons of relative accuracy and cost effectiveness are given in section 8.

a. Alternating direction scheme, MACHO

One possibility is to simply begin with an x-direction *advective-form* flux-difference intermediate update in the first step—being careful not to overwrite the "old" $\bar{\phi}$ values:

$$\bar{\phi}_{AX} = \bar{\phi} + X_A(\bar{\phi}). \tag{32}$$

Then use $\bar{\phi}_{AX}$ for the calculation of the subsequent y-direction *conservative-form* flux-difference (thereby introducing the stabilizing cross terms), combined with a separate additional conservative-form flux difference in the x direction (based on the *original* $\bar{\phi}$ values). This gives an equivalent overall update of the form

$$\bar{\phi}^{+}_{XY} = \bar{\phi} + X_C(\bar{\phi}) + Y_C(\bar{\phi}_{AX}), \tag{33}$$

or, expanding the implied operations,

$$\bar{\phi}^{+}_{XY} = (1 + X_C + Y_C + Y_C X_A)(\bar{\phi}). \tag{34}$$

Each flux-difference calculation is one-dimensional, but this form clearly satisfies conservation and maintains constancy, while allowing the potential for stability through the advective-conservative hybrid cross-coupling term. In the next time step, the coordinate-direction sequence is reversed,

$$\bar{\phi}^{+}_{YX} = \bar{\phi} + X_C(\bar{\phi}_{AY}) + Y_C(\bar{\phi}) \tag{35}$$

or

$$\bar{\phi}^{+}_{YX} = (1 + X_C + Y_C + X_C Y_A)(\bar{\phi}). \tag{36}$$

The algorithm then alternates between Eqs. (33) and (35). We call this the "multidimensional advective-conservative hybrid operator" or MACHO method.

The need for the alternating direction aspect of MACHO is demonstrated in Fig. 2, showing the well-known problem of pure advection of an initial Gaussian distribution in an advection field equivalent to (anticlockwise) solid-body rotation. For the cases shown, the one-dimensional fluxes are computed using an unlimited fifth-order NIRVANA formulation. [One needs to take care in drawing general conclusions when using this test velocity field because the x-component velocity is not a function of x and the y component is not a function of y; thus, for example, a conventional entirely conservative-form operator-splitting method will *not* show any lumpiness due to splitting error (i.e., a constant is maintained, exactly); similarly, a conventional entirely advective-form operator-splitting method will *appear* to be conservative.] Figure 2a shows the results of using Eq. (33) alone; that is, (x followed by y, always).

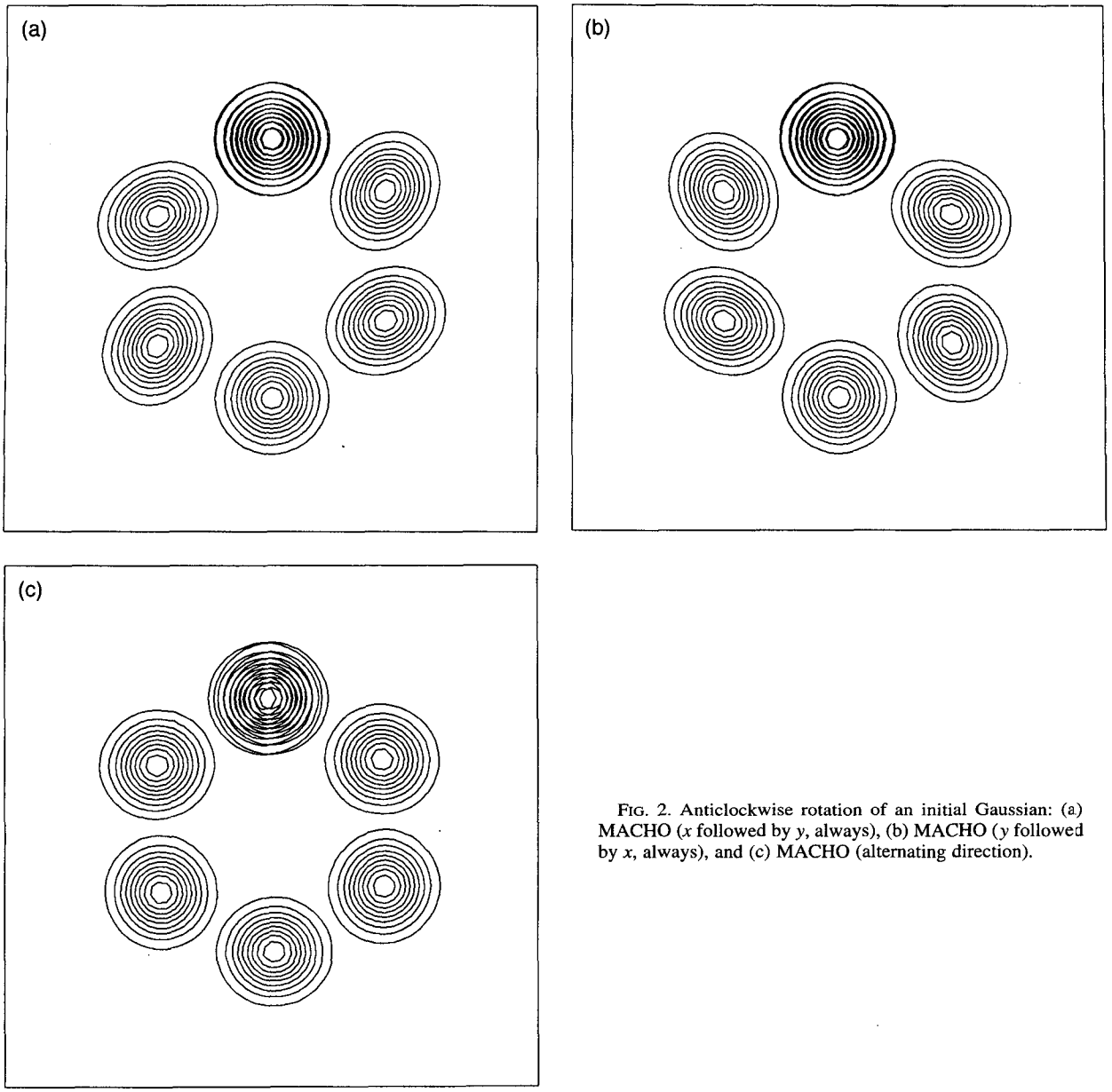

FIG. 2. Anticlockwise rotation of an initial Gaussian: (a) MACHO (x followed by y, always), (b) MACHO (y followed by x, always), and (c) MACHO (alternating direction).

Note the oval-shaped distortion at intermediate locations around the circuit. Distortion in the opposite sense is apparent in Fig. 2b, using Eq. (35) alone; that is, y followed by x, always. The alternating-direction strategy at successive time steps reduces the distortion, as seen in Fig. 2c. In the latter case, there appears to be some "phase lead" using this (relatively large) time step (maximum Courant number component equal to 2π). This is due to the fact that, *in this particular velocity field,* the effective advecting velocities used in the algorithm are always somewhat larger than they should be because they are estimated at a larger radius (imagine approximate linear advective characteristics projected back along a tangent). The apparent phase lead is considerably reduced at smaller time steps. This type of phase error is not usually noticeable in more general velocity fields.

Figure 3 shows the results of using the MACHO strategy applied to the Smolarkiewicz problem, modified as before. Once again, we used unlimited fifth-order one-dimensional NIRVANA fluxes at each step. There is a subtlety involving the most appropriate choice of advective-form transverse velocities; this is described in the next subsection. The constant background field is clearly maintained, but the com-

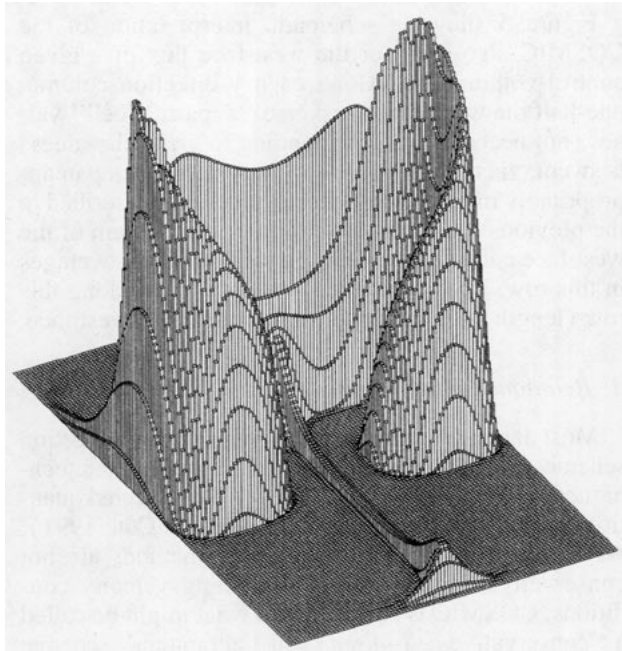

FIG. 3. Alternating-direction MACHO results for the raised Smolarkiewicz test problem at $t = 3T/200$.

putation is absolutely conservative—the sum of computed $\bar{\phi}$ values over all cells remains constant, to machine accuracy. For reference, Fig. 4 shows results for an alternating-direction entirely advective-form calculation (also using an unlimited fifth-order NIRVANA formulation). Superficially, results appear quite good; although, as discussed in section 8, the error is significantly larger than that of the MACHO calculation.

More importantly, however, this test demonstrates that the conventional advective-form calculation is not conservative. We have tracked the sum of computed $\bar{\phi}$ values as a function of time, for both MACHO and the fully advective-form computation. For MACHO, this diagnostic remains constant to machine accuracy, as mentioned above. For the advective-form scheme, it drifts down continually, losing about 4% of the total "mass" even over the relatively short time period, $t = 3T/200$. The nonconservative drift is a function of the advecting velocity field (as pointed out above, solid-body rotation does not introduce such a drift in total "mass"). For general velocity fields occurring in practical problems, the drift could be positive (anomalous gain in "mass") or negative (anomalous loss of "mass"). Although proponents of nonconservative methods (particularly semi-Lagrangian schemes) tend to minimize the seriousness of lack of conservation, it clearly could be an important consideration in some types of problems. The need for strict conservation (combined with no time-step restrictions, other than those dictated by accuracy considerations) has been a motivating factor in developing the various advection schemes described in this paper.

b. *Appropriate transverse velocities*

Assume that normal velocities are known on each face, so that Eq. (9) is satisfied exactly. For the advective-form step (which generates the necessary transverse cross-coupling), we need to choose an appropriate cell-based velocity, as in Eq. (16), for example. The simplest way to do this would be to average c_{xw} and c_{xe} for c_x^{cell} (or c_{ys} and c_{yn} for c_y^{cell}). In other words, use average *cell-centered* velocity components. This method would, however, sometimes generate a spurious flux across dividing streamlines (e.g., if the dividing streamline lies along a cell face) near regions where the transverse component changes sign, so the following simple strategy has been employed:

For a y-direction advective-form update (representing a transverse contribution to a subsequent x-direction conservative-form flux estimate),

(i) if $c_{yn} > 0$ and $c_{ys} \geqslant 0$, set $c_y^{\text{cell}} = c_{ys}$;
(ii) if $c_{yn} \leqslant 0$ and $c_{ys} < 0$, set $c_y^{\text{cell}} = c_{yn}$;
(iii) otherwise, if $c_{ys}c_{yn} < 0$, set $c_y^{\text{cell}} = 0$.

An entirely analogous procedure is used, of course, for the x-direction advective-form contribution to the y-direction flux. We have experimented with other transverse-velocity strategies but, to date, the above procedure seems to work best in practice.

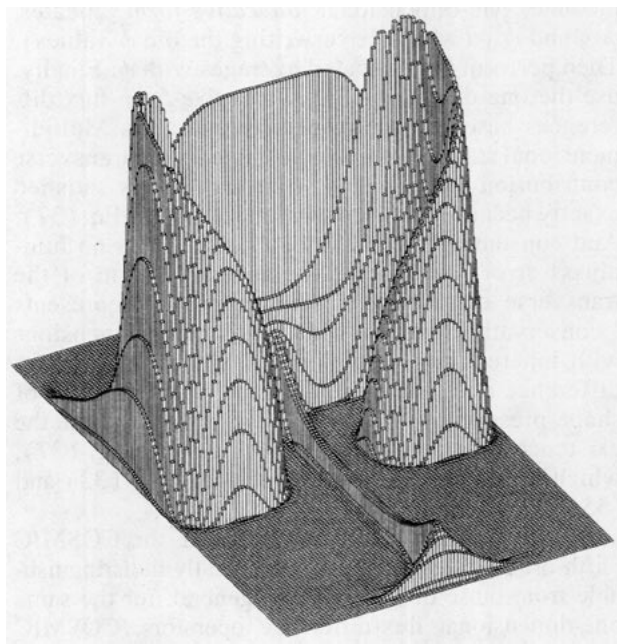

FIG. 4. Conventional alternating-direction advective-form operator-splitting results for the raised Smolarkiewicz test problem at $t = 3T/200$.

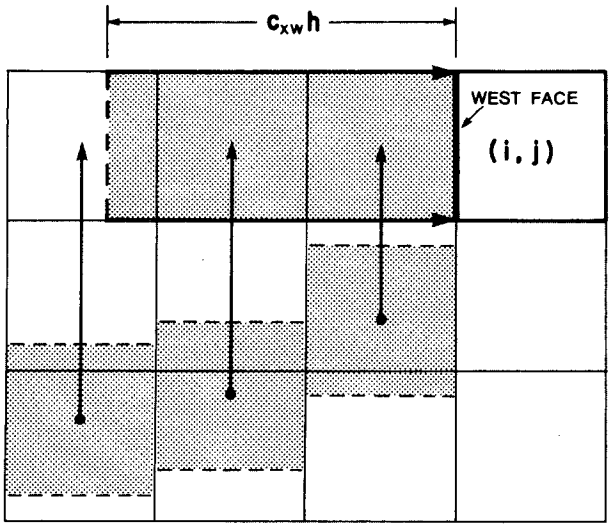

FIG. 5. Schematic interpretation of the COSMIC algorithm for the west-face flux of a control volume.

c. Symmetric form, COSMIC

Assume that the flux-difference operators in Eqs. (33) and (35) are linear, and average the two equations. This gives a symmetric form

$$\bar{\phi}^{+} = \bar{\phi} + X_C\left[\frac{1}{2}(\bar{\phi} + \bar{\phi}_{AY})\right] + Y_C\left[\frac{1}{2}(\bar{\phi} + \bar{\phi}_{AX})\right]. \tag{37}$$

In this case, we first compute and store two intermediate one-dimensional *advective-form* updates, $\bar{\phi}_{AX}$ and $\bar{\phi}_{AY}$ (without overwriting the old $\bar{\phi}$ values). Then perform the indicated averages with $\bar{\phi}$. Finally, use the one-dimensional *conservative-form* flux differences based on the respective averages. Multidimensional stability is made possible by the transverse contribution to each flux. Conservation is satisfied exactly because of the conservative form of Eq. (37). And constancy is maintained (i.e., there is no lumpiness error) because of the advective form of the transverse contributions. This approach represents "conservative operator splitting for multidimensions with inherent constancy" or COSMIC. If the flux-difference operators are nonlinear (such as those of shape-preserving schemes), we simply postulate the existence of a symmetric form given by Eq. (37), which happens to be consistent with Eqs. (33) and (35) in the linear case.

For the Smolarkiewicz test problem, the COSMIC (fifth-order) calculations are graphically indistinguishable from those of MACHO. In general, for the same one-dimensional flux-difference operators, COSMIC tends to be somewhat more accurate than MACHO—but also a little more expensive. The relative computational efficiency is explored in section 8.

Figure 5 shows a schematic interpretation of the COSMIC algorithm for the west-face flux of a given control-volume cell. Along each y-direction column, one-half the weight of transverse "departure cell" values (not necessarily corresponding to *grid* cell values) is swept, via the advective-form operator (using an appropriately modified cell-based velocity as described in the previous subsection), into the row upstream of the west face and added to half the weight of cell averages in this row. The appropriate amount of flux along this row (length $c_{xw}h$) is then swept through the west face.

d. Relationship to other schemes

Most large-Δt explicit multidimensional advection schemes are currently based on semi-Lagrangian techniques, interpolating point values of the advected quantity at the departure point (Staniforth and Côté 1991). As is well known, semi-Lagrangian methods are not conservative. Under *uniform* advecting velocity conditions, COSMIC is *equivalent* to what might be called a "conservative *cell-based* semi-Lagrangian" scheme. The updated "arrival cell" value on an Eulerian grid at cell (i, j) is *effectively* set equal to the earlier "departure cell" average value. Details of this relationship are discussed in appendix B. Of course, the actual algorithm follows the strictly conservative flux-difference form given by Eq. (37). This interpretation also helps to explain the inherent "stability" of the scheme for any Δt. The MACHO scheme has a similar interpretation. By contrast, the unstable simple-minded update given by Eq. (25) has no such interpretation.

In addition to the relationship to semi-Lagrangian schemes, there is a strong resemblance between COSMIC and our large-time-step conservative ENIGMATIC scheme (Leonard et al. 1995c). For Courant

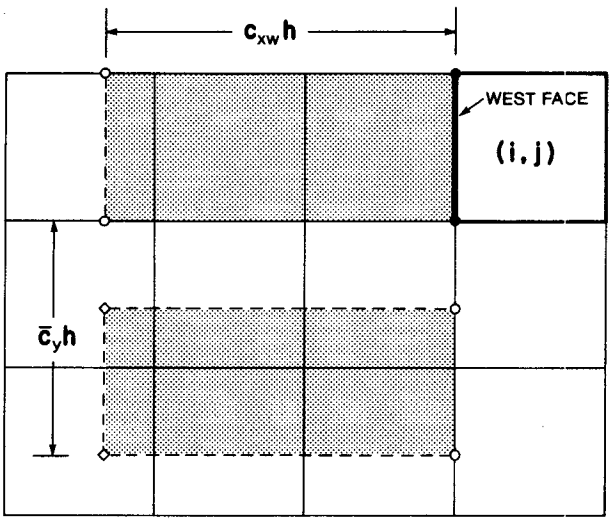

FIG. 6. Schematic interpretation of the ENIGMATIC algorithm for the west-face flux of a control volume.

number components less than 1, there are also strong similarities between COSMIC and our flux-integral method, FIM (Leonard et al. 1995b).

Figure 6 shows a schematic of the ENIGMATIC calculation of the west-face flux for cell (i, j). The *only* difference between this and the COSMIC flux depicted in Fig. 5 is that, for ENIGMATIC, a *single* average transverse velocity, $\bar{c}_y$ in the figure, is assumed for any given face, whereas for COSMIC, transverse velocities used for a particular row of cells upstream from the west face vary from column to column (as indicated in Fig. 5).

The relationship between COSMIC and the FIM is most clearly seen in the case of a first-order FIM (which, of course, is not recommended for actual use because of the gross inherent artificial numerical diffusion associated with such a method; it is used here simply as an illustrative example). For $c_{xw}(i, j)$ and $c_{ys}(i-1, j)$ both positive (and less than 1), the west-face advection flux is calculated by integrating the subcell $\phi(x, y)$ over the flux-integral parallelogram shown in Fig. 7. To avoid a cumbersome notation, the Courant number components are written as c_{xw} and c_{ys}^-, respectively. For a first-order scheme, the subcell behavior is piecewise constant (equal to the local cell-average value over each individual cell). Clearly, from Fig. 7, we see that the integral can be broken up into rectangular and triangular areas, each involving a constant subcell value. The individual contributions to the integral are then proportional to the areas involved multiplied by the respective cell-average value. This means that the flux is, in this case,

$$c_{xw}\phi_w^{\text{eff}} = \underset{\begin{pmatrix}\text{rectangle}\\ 1\,2\,4\,7\,1\end{pmatrix}}{c_{xw}\bar{\phi}_{i-1,j}} - \underset{\begin{pmatrix}\text{top triangle}\\ 1\,2\,3\,1\end{pmatrix}}{\frac{c_{xw}c_{ys}^-}{2}\bar{\phi}_{i-1,j}} + \underset{\begin{pmatrix}\text{bottom triangle}\\ 7\,4\,5\,7\end{pmatrix}}{\frac{c_{xw}c_{ys}^-}{2}\bar{\phi}_{i-1,j-1}} \quad (38)$$

or, factoring out the normal Courant number component,

$$c_{xw}\phi_w^{\text{eff}} = c_{xw}\left[\bar{\phi}_{i-1,j} + \frac{c_{ys}^-}{2}(\bar{\phi}_{i-1,j-1} - \bar{\phi}_{i-1,j})\right]. \quad (39)$$

This can be rewritten as

$$c_{xw}\phi_w^{\text{eff}} = c_{xw}\left\{\frac{1}{2}\bar{\phi}_{i-1,j} + \frac{1}{2}[\bar{\phi}_{i-1,j} + c_{ys}^-(\bar{\phi}_{i-1,j-1} - \bar{\phi}_{i-1,j})]\right\} \quad (40)$$

or

$$c_{xw}\phi_w^{\text{eff}} = c_{xw}\left\{\frac{1}{2}[\phi_w^{\text{DC}}(\bar{\phi}) + \phi_w^{\text{DC}}(\bar{\phi}_{AY})]\right\} = c_{xw}\phi_w^{\text{DC}}\left[\frac{1}{2}(\bar{\phi} + \bar{\phi}_{AY})\right], \quad (41)$$

where "DC" stands for a (first-order) *one-dimensional* donor-cell value at the indicated face, and $\bar{\phi}_{AY}$ is the *advective-form* update in the transverse direction; in this case,

$$\bar{\phi}_{AY} = \bar{\phi}_{i-1,j} + c_{ys}^-(\bar{\phi}_{i-1,j-1} - \bar{\phi}_{i-1,j}). \quad (42)$$

The important thing to note is that the *same* transverse velocity component, c_{ys}^- in Eq. (42), multiplies both the north and the south (donor-cell) face values for cell $(i-1, j)$. Equation (41) is identical in form to a *first-order* COSMIC formula for positive Courant number components less than 1. Higher-order FIM formulas can be interpreted in a similar manner. The interesting (and important) thing, of course, is that whereas the FIM formulation is limited to small Δt ($|c_x|, |c_y| \leq 1$), COSMIC has no such Δt restrictions.

As mentioned earlier, the COSMIC scheme described here is similar in many respects to the so-called "flux-form semi-Lagrangian" method recently devised by Lin and Rood (1996). For the transverse advective-form contribution, these authors recommend cell-centered velocities and appear to advocate a simple first-order method, using a higher-order conservative-form scheme for the overall update. However, as they demonstrate, their method can be extended to include higher-order transverse contributions, as well, similar to the methods described here.

e. *Pseudodensity algorithm*

Yet another method exhibiting strict conservation and constancy preservation can be designed by introducing a pseudodensity and using conservative-form one-dimensional flux-difference calculations at each step. This is related to a technique described by Easter (1993).

In this case we begin with a *conservative*-form one-dimensional update in the x direction, with the face values based on $\bar{\phi}$,

$$\bar{\phi}_{CX} = \bar{\phi} + c_{xw}\phi_w^{\text{1D}}(\bar{\phi}) - c_{xe}\phi_e^{\text{1D}}(\bar{\phi}). \quad (43)$$

Now introduce a pseudodensity, initially set equal to 1 everywhere (and reset to 1 before each update). A conservative-form, x-direction update of this pseudodensity would give

$$\bar{\rho}_{CX} = 1 + c_{xw} - c_{xe}. \quad (44)$$

The corresponding pseudoscalar, at this stage, is

$$\bar{\phi}_{CX}^* = \frac{\bar{\phi}_{CX}}{\bar{\rho}_{CX}}. \quad (45)$$

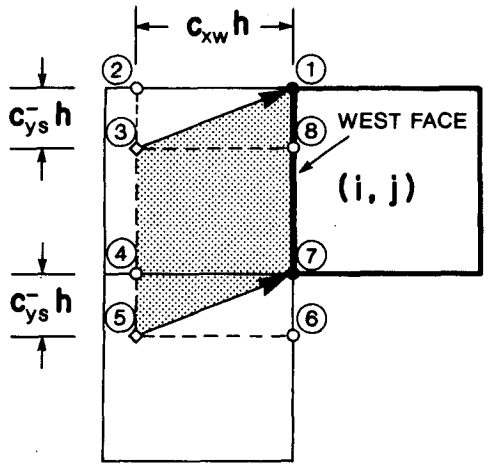

FIG. 7. West-face flux for a first-order flux integral method for (positive) Courant number components less than 1.

This is now used for estimating one-dimensional north and south face values in the subsequent y-direction update

$$\bar{\phi}^{+}_{CXY} = \bar{\phi}_{CX} + c_{ys}\phi_s^{1D}(\bar{\phi}^{*}_{CX}) - c_{yn}\phi_n^{1D}(\bar{\phi}^{*}_{CX}). \quad (46)$$

Note that the first term on the right-hand side is $\bar{\phi}_{CX}$ (and not $\bar{\phi}^{*}_{CX}$). As with MACHO, the directional sequence is reversed at the next time step. The overall update is conservative because face fluxes are unique to each face. Constancy is also maintained, as seen by setting $\bar{\phi} \equiv \bar{\phi}_0$ initially, in which case Eq. (43) becomes

$$\bar{\phi}_{CX} = (1 + c_{xw} - c_{xe})\bar{\phi}_0, \quad (47)$$

giving, from Eq. (45),

$$\bar{\phi}^{*}_{CX} = \frac{\bar{\phi}_{CX}}{1 + c_{xw} - c_{xe}} \equiv \bar{\phi}_0. \quad (48)$$

In other words, the potential lumpiness in the scalar is exactly cancelled by the identical lumpiness in the pseudodensity.

A symmetric form analogous to COSMIC is easily devised. Starting with temporary conservative-form updates in each direction, form the following pseudoscalars and concomitant averages

$$\bar{\phi}^{*}_{CX} = \frac{\bar{\phi}_{CX}}{1 + c_{xw} - c_{xe}} \quad (49)$$

$$\bar{\phi}_{AVX} = \tfrac{1}{2}(\bar{\phi} + \bar{\phi}^{*}_{CX}) \quad (50)$$

$$\bar{\phi}^{*}_{CY} = \frac{\bar{\phi}_{CY}}{1 + c_{ys} - c_{yn}} \quad (51)$$

$$\bar{\phi}_{AVY} = \tfrac{1}{2}(\bar{\phi} + \bar{\phi}^{*}_{CY}). \quad (52)$$

Then the single-step conservative update becomes

$$\bar{\phi}^{+} = \bar{\phi} + c_{xw}\phi_w^{1D}(\bar{\phi}_{AVY}) - c_{xe}\phi_e^{1D}(\bar{\phi}_{AVY}) + c_{ys}\phi_s^{1D}(\bar{\phi}_{AVX}) - c_{yn}\phi_n^{1D}(\bar{\phi}_{AVX}). \quad (53)$$

This pseudodensity strategy gives results very similar to those of MACHO or COSMIC.

6. Three-dimensional algorithms

The MACHO strategy can be applied directly to three dimensions. To reduce directional bias, one should use a consistent sequence of each of the six possible permutations of the order in which the coordinate directions are considered in turn.

To construct a three-dimensional COSMIC scheme, consider the average of the six permutations of the product of each of the operators $(1 + X)$, $(1 + Y)$, and $(1 + Z)$. This can be written as

$$\begin{aligned}\text{AVERAGE} &= 1 + X\left[1 + \frac{1}{2}Y\left(1 + \frac{1}{3}Z\right) + \frac{1}{2}Z\left(1 + \frac{1}{3}Y\right)\right] \\ &+ Y\left[1 + \frac{1}{2}Z\left(1 + \frac{1}{3}X\right) + \frac{1}{2}X\left(1 + \frac{1}{3}Z\right)\right] \\ &+ Z\left[1 + \frac{1}{2}X\left(1 + \frac{1}{3}Y\right) + \frac{1}{2}Y\left(1 + \frac{1}{3}X\right)\right].\end{aligned} \quad (54)$$

This operator applied to $\bar{\phi}$ can then be rearranged to give the following three-dimensional COSMIC update:

$$\begin{aligned}\bar{\phi}^{+} = \bar{\phi} &+ X_C\left\{\frac{1}{6}[(\bar{\phi} + \bar{\phi}_{AY} + \bar{\phi}_{AYZ}) + (\bar{\phi} + \bar{\phi}_{AZ} + \bar{\phi}_{AZY})]\right\} \\ &+ Y_C\left\{\frac{1}{6}[(\bar{\phi} + \bar{\phi}_{AZ} + \bar{\phi}_{AZX}) + (\bar{\phi} + \bar{\phi}_{AX} + \bar{\phi}_{AXZ})]\right\} \\ &+ Z_C\left\{\frac{1}{6}[(\bar{\phi} + \bar{\phi}_{AX} + \bar{\phi}_{AXY}) + (\bar{\phi} + \bar{\phi}_{AY} + \bar{\phi}_{AYX})]\right\},\end{aligned} \quad (55)$$

where, for example,

$$\bar{\phi}_{AYZ} = \bar{\phi}_{AZ}(\bar{\phi}_{AY}) = \bar{\phi}_{AY} + Z_A(\bar{\phi}_{AY}). \quad (56)$$

The algorithm thus proceeds as follows:

(i) Compute and store the three basic *advective*-form updates $\bar{\phi}_{AX}$, $\bar{\phi}_{AY}$, and $\bar{\phi}_{AZ}$.

(ii) Compute and store the six cross-coupling *advective*-form updates $\bar{\phi}_{AXY}$, $\bar{\phi}_{AYX}$, $\bar{\phi}_{AYZ}$, $\bar{\phi}_{AZY}$, $\bar{\phi}_{AZX}$, and $\bar{\phi}_{AXZ}$.

(iii) Compute and store the three averages defined within the respective curly brackets in Eq. (55). Call these, for example, $\bar{\phi}_{AVYZ}$, $\bar{\phi}_{AVZX}$, and $\bar{\phi}_{AVXY}$, respectively.

(iv) The single-step explicit update then uses *conservative*-form one-dimensional flux differences based on the respective averages:

$$\bar{\phi}^+ = \bar{\phi} + X_C(\bar{\phi}_{AVYZ}) + Y_C(\bar{\phi}_{AVZX}) + Z_C(\bar{\phi}_{AVXY}). \tag{57}$$

Note how this reverts to Eq. (37) for two-dimensional flow if, for example, all z-direction fluxes are zero so that

$$\bar{\phi}_{AZ} = \bar{\phi} \tag{58}$$

and

$$\bar{\phi}_{AYZ} = \bar{\phi}_{AZY} = \bar{\phi}_{AY}. \tag{59}$$

7. Shape preservation

Piecewise-polynomial (or spline) techniques used in the one-dimensional flux calculations can lead to unphysical undershoots or overshoots of the transported variable in regions involving strong changes in gradient. This is a type of Gibbs phenomenon, reflecting the fact that polynomials are not appropriate interpolators for data involving nearly discontinuous behavior. Undershoots, for example, can be found in Fig. 3 for the MACHO calculation (using *unlimited* piecewise-fifth-order polynomial interpolation in each of the one-dimensional NIRVANA flux calculations). In many cases, it is important to try to eliminate (or at least minimize) this lack of shape preservation; in particular, normalized density ratios should lie between 0 and 1; in other situations (e.g., turbulence modeling), a local anomalously negative quantity (caused by a spurious numerical undershoot) could lead to nonlinear instability.

For small time steps, usually governed by either

$$|c_x| + |c_y| \leq 1 \tag{60}$$

or

$$\max(|c_x|, |c_y|) \leq 1, \tag{61}$$

a number of flux-limiter approaches can be used. One of the most successful of these appears to be the strategy recently developed by Thuburn (1996). This is a genuinely multidimensional flux-limiter technique, closely related to our own multidimensional limiter efforts (Leonard et al. 1993). Many other workers have applied the flux-corrected transport (FCT) idea of Zalesak (1979); for example, see Hólm (1995). This involves modifying first-order upwind fluxes with limited antidiffusive fluxes. The first-order flux is usually taken to be the one-dimensional donor-cell form, governed by inequality (60) (Rasch 1994). Hólm appears to be the first to have used a multidimensional first-order scheme for FCT; this is governed by the less restrictive condition given by inequality (61) (see Leonard et al. 1993).

For large Δt and deformational velocity fields, shape-preserving techniques appear to be more elusive. For example, even first-order conservative-form operator-splitting schemes are no longer monotonic for Courant number components larger than one. Thus FCT techniques cannot be used. Using entirely *advective*-form operator splitting (e.g., based on shape-preserving one-dimensional schemes such as NIRVANA), multidimensional shape preservation can be achieved. But, of course, conservation is lost. By contrast, conservative constancy-preserving schemes, such as MACHO or COSMIC, cannot guarantee *strict* multidimensional shape preservation under all circumstances. The problem stems from a combination of large Δt and deformational velocity fields. Figure 8 shows an alternating-direction MACHO calculation of the well-known "rotating split cylinder" problem, using seventh-order NIRVANA fluxes in combination with the large-Δt universal limiter (Leonard et al. 1995a; Leonard 1991); the maximum Courant number component is 2π. The figure shows a histogram of cell-average initial conditions (which also represents the exact solution after any integer number of rotations) and computed cell-average results after one rotation. The computation is performed on a 100 cell $\times$ 100 cell domain; the cylinder, initially centered at $(50h, 75h)$ is of radius $15h$, with a 5 cell $\times$ 25 cell slot; only the 50 cell $\times$ 50 cell region near the cylinder is shown in the figure. Results are shape preserving but this is because, for this particular velocity field (as explained earlier), MACHO is equivalent to conventional (but conservative) entirely advective-form operator splitting. The exceptionally sharp resolution seen in the figure is due primarily to the high-order base scheme used for the one-dimensional fluxes.

Figure 9 shows results for the Smolarkiewicz problem using conventional advective-form operator splitting (with *limited* fifth-order NIRVANA one-dimensional fluxes using cell-based velocity components as previously described). This should be compared with Fig. 4. Results are shape preserving—but not conservative. Finally, Fig. 10 shows "limited" MACHO results for a relatively large time step (again using a limited fifth-order NIRVANA formulation). Although undershoots appear to be eliminated in comparison with the corresponding unlimited scheme (Fig. 3), they are not completely eliminated (the magnitude of the maximum undershoot in Fig. 10 is 0.0021—a very small, but not totally negligible, value). This appears to be a problem with all large-Δt conservative schemes in general velocity fields. However, since the lack of

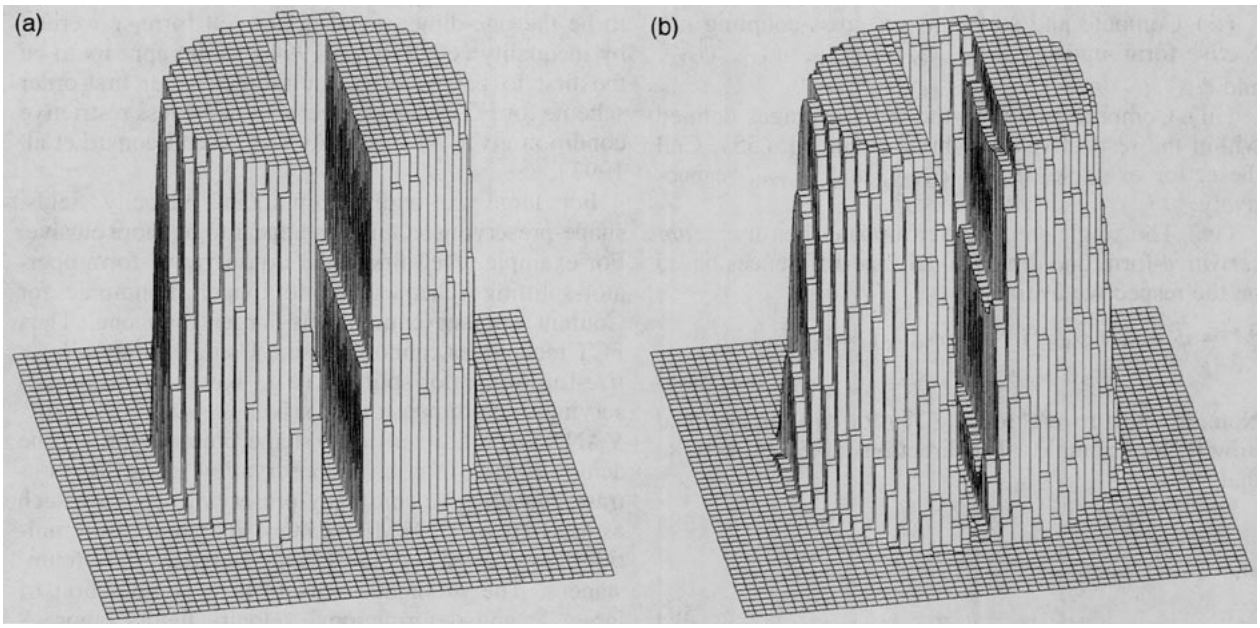

FIG. 8. MACHO calculation of the rotating split cylinder problem, using seventh-order NIRVANA fluxes and the universal limiter. (a) Cell-average initial conditions. (b) Cell-average results after one rotation.

shape preservation appears to be quite small, such schemes are appropriately called ESP.

8. Computational efficiency

In this section, we present a preliminary study of the relative cost and accuracy of the new advection schemes introduced in this paper. In particular, we first perform a spatial grid-refinement study using the Smolarkiewicz problem, keeping the time step fixed. We also track the relative cost of the various new schemes based on CPU times. Of particular interest is the computational efficiency diagram: a plot (on a log–log scale) of error versus cost for different methods, as the grid is refined. We use an L_1 error norm

$$L_1 = \frac{h^2}{L^2} \sum_i \sum_j |\bar{\phi}_{\text{computed}} - \bar{\phi}_{\text{exact}}|. \qquad (62)$$

Clearly, other diagnostics such as L_2 or L_∞ could be used. This diagram gives a good indication of the "best" (most cost-effective) scheme for a class of problems similar to the test problem being studied. Specifically, we can see at a glance which scheme has the lowest cost for a prescribed accuracy or, alternatively, which scheme achieves the best accuracy within a prescribed budget.

Figure 11 shows the computational efficiency diagram for COSMIC and the alternating-direction entirely advective-form operator-splitting technique given by Eqs. (23) and (24). Both schemes use unlimited fifth-order NIRVANA formulations. The results presented are at output times incremented by $T/200$; the grid spacings are given by $h = 0.25$, 0.5, 1, and 2 units. The time step in each case is $\Delta t = 1.32$. Respective maximum component Courant numbers are 5.28, 2.64, 1.32, and 0.66. Note that at fine spatial resolution, the error is leveling out; the asymptote represents the temporal discretization error, in respective cases.

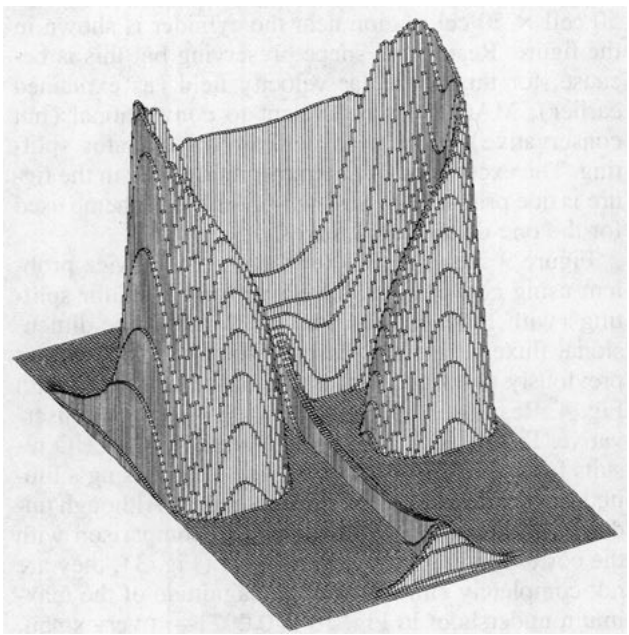

FIG. 9. Entirely advective-form alternating-direction operator-splitting results for the Smolarkiewicz test problem, using limited fifth-order NIRVANA fluxes; $t = 3T/200$.

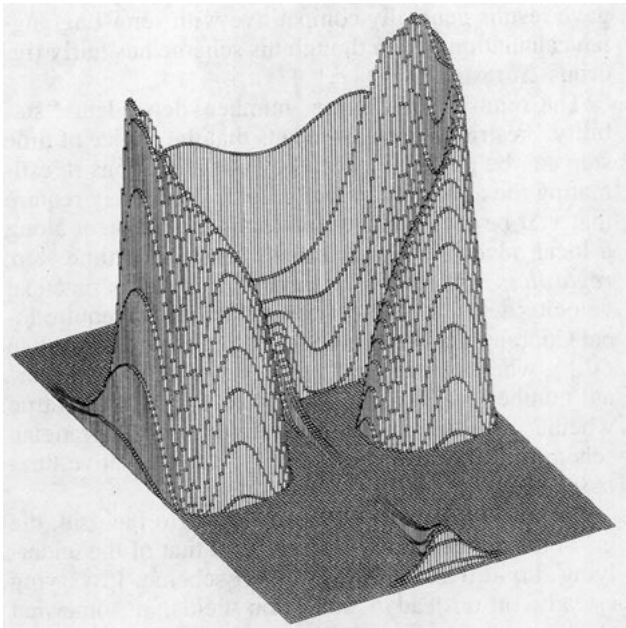

FIG. 10. Alternating-direction MACHO results for the Smolarkiewicz test problem, using limited fifth-order NIRVANA fluxes; $t = 3T/200$.

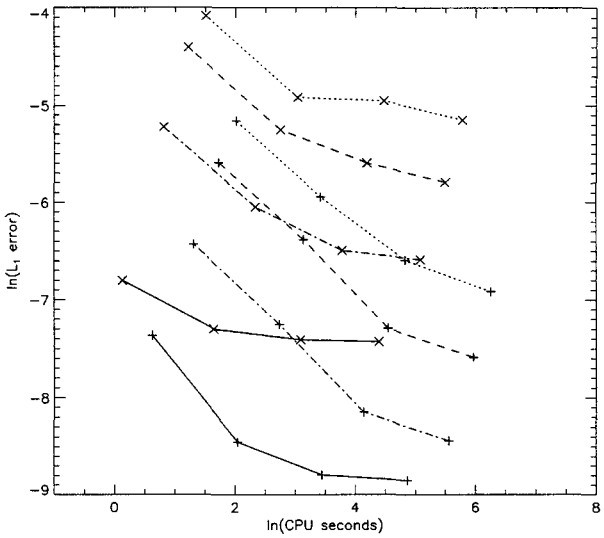

FIG. 11. Computational efficiency diagram for COSMIC (+) and the alternating-direction advective-form operator-splitting technique (×). The lines join up results at the same time for different resolutions; solid lines are at $t = T/200$, dash–dot for $t = 2T/200$, dashed for $t = 3T/200$, and dotted for $t = 4T/200$.

It is now immediately obvious that, while the conventional advective-form scheme is nearly 50% less expensive to run (per space–time grid point), the error is substantially larger, irrespective of the question of conservation. Thus, if one were to specify a required accuracy, in terms of L_1 error, at time $t = 3T/200$, of no larger than, say, 3.3×10^{-3} (or $\approx e^{-5.7}$), then COSMIC would cost roughly 7 CPU seconds ($\approx e^{1.9}$), whereas the advective-form scheme would cost 122 CPU seconds ($\approx e^{4.8}$). For a prescribed accuracy, then, the (nonconservative) advective-form operator-split scheme is appallingly expensive in comparison with COSMIC. Alternatively, for a prescribed computational budget, COSMIC is able to produce results with significantly lower error.

Figure 12 shows the same diagram for COSMIC again, but now plotted with alternating-direction MACHO and the alternating-direction basic and the symmetrical forms of the pseudodensity-compensated conservative-form operator-splitting technique given by Eqs. (46) and (53). All schemes use fifth-order one-dimensional NIRVANA fluxes. Beyond the first output time ($t = T/200$), a steady pattern of the results has emerged. At high resolution, there is very little to choose between any of the schemes (a particular required accuracy would cost much the same) although COSMIC is fractionally the most efficient. At lower resolutions, it can be seen that all the schemes are generating very similar errors at each time and resolution, and so the schemes that are less expensive on a space–time gridpoint basis are similarly more computationally efficient. The costs of the schemes, relative to a COSMIC value of 1.0, are as follows: basic pseudodensity conservative form, 0.43; MACHO, 0.7; and symmetrical pseudodensity conservative-form, 0.85.

Finally, Fig. 13 shows the computational efficiency diagram for COSMIC schemes using one-dimensional NIRVANA fluxes of various orders (third, fifth, and seventh). In this case, Δt is changed in proportion to

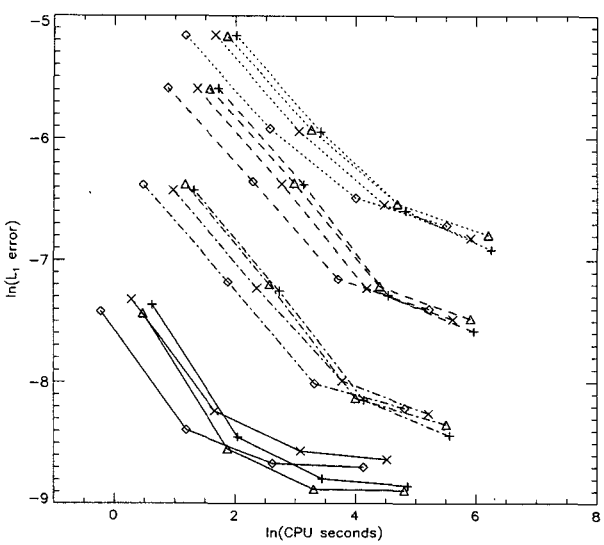

FIG. 12. Computational efficiency diagram for COSMIC (+), and alternating-direction forms of MACHO (×) and the basic (◇) and symmetrical (△) pseudodensity operator-splitting methods. The lines are as in Fig. 11.

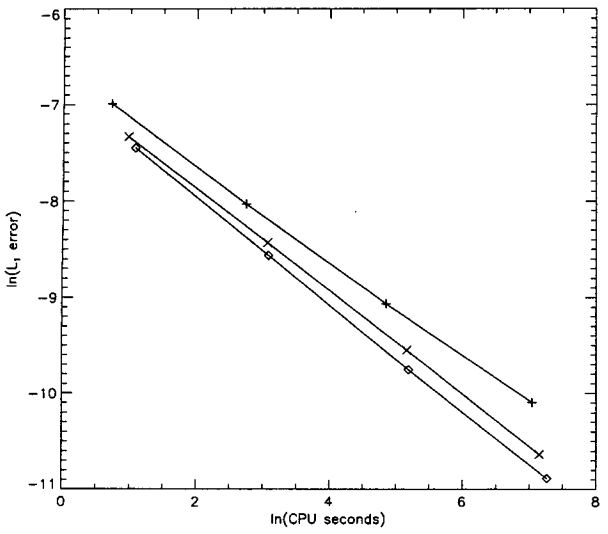

FIG. 13. Computational efficiency diagram for COSMIC schemes of various orders: third order (+), fifth order (×), and seventh order (◇). Results are for $t = T/200$.

h ($\Delta t/h = 0.51$). Note that although cost increases with order on a fixed mesh, accuracy increases even more, so that the higher-order schemes are more cost effective, overall: lower cost for a prescribed accuracy, or better accuracy for a prescribed cost. In our experience, this appears to be a general trend (Leonard and MacVean 1995).

9. Conclusions

Our primary aim has been to take recent developments in extending explicit, flux-based one-dimensional advection algorithms to (potentially) arbitrarily large time step, and apply them to multidimensions without generating the negative "side effects" of conventional operator-splitting methods. In general terms, we have tried to "do operator splitting correctly," using combinations of advective-form and conservative-form unrestricted-time-step explicit one-dimensional operators—maintaining conservation without introducing splitting-error lumpiness. The resulting algorithms should be easily incorporated into existing codes based on traditional operator-splitting methods.

The new advection schemes, MACHO and COSMIC (and their pseudodensity relatives), should be competitive with popular large-Δt semi-Lagrangian schemes—except, of course, that now we have the important added advantage of strict conservation. We have not performed direct computational-efficiency comparisons between the new methods and semi-Lagrangian schemes (primarily because of subtle complications arising from the difference between nodal-point and cell-average formulations). But we extrapolate from the conclusions of Rasch (1994), who found that his nominally third-order conservative scheme gave results generally competitive with semi-Lagrangian calculations, even though his scheme has fairly rigorous Δt restrictions ($|c_x| + |c_y| \lesssim 1$).

The removal of Courant number–dependent "stability" restrictions on Δt means that the choice of time step can be guided by accuracy considerations in estimating the advecting velocity field. We merely require that $\mathbf{v}\Delta t$ be a "good" estimate of displacement along a local advective characteristic in a single time step, *regardless of the Eulerian mesh size.* Thus, in practical velocity fields, a coarse-mesh region might require local Courant number components significantly less than $O(1)$, whereas fine-mesh regions might involve Courant numbers very much larger than $O(1)$. This is true whether one uses (nonconservative) semi-Lagrangian schemes or the new unrestricted-Δt conservative flux-based methods.

For uniform advection at any angle to the grid, the grid-convergence rate is the same as that of the underlying flux-difference interpolation scheme. In varying (steady or unsteady) advection fields, a somewhat slower spatial convergence rate is typical; this appears to be due to phase errors arising from the estimation of the advecting velocity components. However, for flows involving unsteady velocities, the temporal convergence rate is only first order—if lagged advecting velocities are used. In general, the truncation error would then involve terms of the form

$$\mathrm{TE} = O(|u|h^n, \Delta t^n), \tag{63}$$

where n is the formal order of the constant-coefficient scheme. But the velocity components themselves have the form

$$|u| = |u_0|[1 + O(\Delta t)]. \tag{64}$$

Thus, for example, in a grid-convergence study holding Δt proportional to h (approximately constant Courant number), the grid convergence rate is (close to) $O(h^n)$. If Δt is constant, the convergence rate (relative to the solution for $h \to 0$ at this Δt) is also $O(h^n)$. But if h is held constant, the temporal convergence rate is only $O(\Delta t)$. In our experience, this does not seem to represent a serious problem. Better temporal convergence can be achieved by staggering the velocity field in time as is done with conventional operator-splitting methods and many semi-Lagrangian and other schemes. However, as with any large-Δt scheme, one needs to give careful thought to the choice of time step.

The new advection schemes described here, in common with our earlier ENIGMATIC scheme, are essentially shape preserving (ESP) in the following sense. If the component Courant numbers are everywhere less than one and the individual (advective and conservative) one-dimensional fluxes are based on shape-preserving interpolation—such as that corresponding to the universal limiter, for example (Leonard 1991), the overall update is shape preserving. However, for large

time steps and general velocity fields (so that the x-component velocity varies with x, and so on), the conservative flux-difference computations in the overall update cannot guarantee shape preservation. Fortunately, in most practical situations, the lack of strict shape preservation appears to be quite small, as was seen to be the case for the Smolarkiewicz test problem. The usefulness of the unrestricted-time-step capability of the schemes will be most apparent in variable-grid applications. For example, on a standard spherical grid where longitudinal mesh refinement occurs near the poles, one would like to choose the time step based on accuracy considerations, so that component Courant numbers are $O(1)$ in coarse-mesh regions; this would imply very large Courant numbers in fine-mesh regions. Under such conditions, ESP behavior appears to occur because in fine-mesh regions, although Courant numbers are high, the velocity field changes very little across any given cell so that the local computation approaches that of an entirely advective-form scheme (which *is* shape preserving provided the individual one-dimensional flux differences are).

A formal stability analysis (e.g., in the von Neumann sense) shows that the large-Δt schemes described here are unconditionally stable under conditions of uniform advection. This can be extended to the entirely advective-form large-Δt scheme, as well. The results follow directly from the large-Δt one-dimensional analysis (Leonard 1994). A demonstration of formal stability in the general case appears to be somewhat more elusive. However, in our experience, using a number of test problems at very large Δt, there is never any hint of instability. As the time step is increased to very large values, accuracy is impaired (because of a less precise estimate of the advective displacement over Δt) but stability remains intact.

Acknowledgments. Part of this research was carried out while the first author was a visiting scientist at the Atmospheric Processes Research Division of the Meteorological Office at Bracknell. The first author also had partial support from a National Science Foundation Mesoscale Dynamic Meteorology Program Grant ATM-9221808. Discussions with John Thuburn of the University of Reading led to the pseudodensity algorithms presented here.

APPENDIX A

Cell-Average Reference Solutions for the Smolarkiewicz Test Problem

This test problem, defined by Smolarkiewicz (1982), is the advection of a scalar field initially in the shape of a cone (of radius 15 units, height normalized here to 1 unit) centered in a square domain of side $L = 100$ units. The advecting flow field is defined by the streamfunction

$$\psi(x, y) = A \sin(kx) \cos(ky), \qquad \text{(A1)}$$

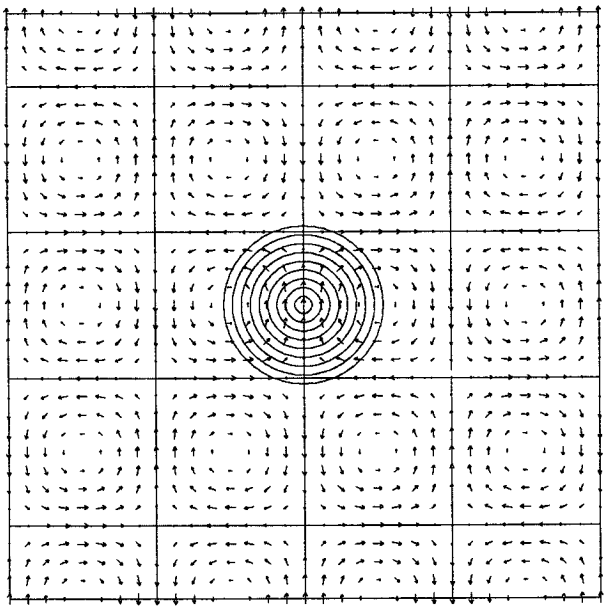

FIG. A1. Velocity field for the Smolarkiewicz test problem. Contour lines show the initial scalar field.

where $A = 8$ and $k = 4\pi/L$, so that the flow consists of a set of symmetrical vortices, as shown in Fig. A1.

Staniforth et al. (1987) showed how the analytic solution for this problem can be derived using the fact that the advected field ϕ is conserved along trajectories. To solve for the trajectories of the fluid elements, they translated the coordinate system (x, y) to one (x', y'), with its origin at the bottom left-hand corner of the square in which the fluid element is constrained; that is, for integer values of n and l,

$$kx = n\pi + \theta \qquad \text{(A2)}$$

$$ky = \left(l - \frac{1}{2}\right)\pi + \lambda, \qquad \text{(A3)}$$

where $\theta = kx'$ and $\lambda = ky'$, so that θ and λ both lie between 0 and π. They then derived equations for the time variation of θ and λ:

$$\left(\frac{d\theta}{dt}\right)^2 = A^2k^4(m - \cos^2\theta) \qquad \text{(A4)}$$

$$\left(\frac{d\lambda}{dt}\right)^2 = A^2k^4(m - \cos^2\lambda), \qquad \text{(A5)}$$

where the constant m can be given in terms of the position of the fluid element at the required time t, that is, (x_t, y_t), by

$$m = 1 - \frac{\psi(x_t, y_t)^2}{A^2}. \qquad \text{(A6)}$$

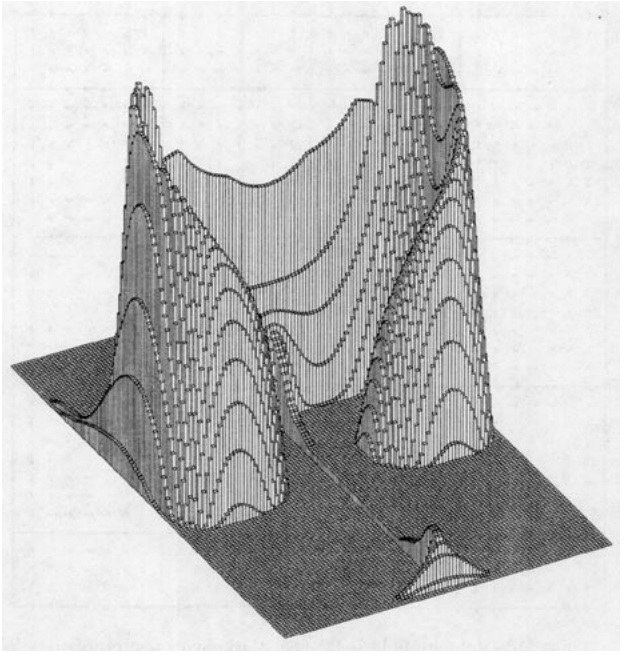

FIG. A2. Two-dimensional histogram of cell-average values of the reference solution for $t = 3T/200$, $h = 0.5$ unit.

Staniforth et al. present analytic solutions at output times $t = T/200$, $2T/200$, $3T/200$, and $4T/200$, where $T = 2637.6$ s; but it should be noted that they work with *nodal-point* values on a highly variable grid with drastically increased resolution in regions of large gradient in the advected field (although they did not point this out, explicitly).

Instead of working with the analytic solution, we prefer to integrate Eqs. (A4) and (A5) numerically (e.g., using a highly accurate fourth-order Runge–Kutta scheme with a very small time step) backward in time to give the initial position (and hence the initial ϕ value) of any prescribed fluid element located at position (x_t, y_t) at time t.

For direct comparison with computed results from finite-volume advection schemes, we present the solution as a histogram of *cell-average* values. A regular grid is used with a spacing of $h = 0.5$ unit (giving 200×200 cells over the whole domain) and staggered so that the bottom left-hand cell is centered at $(0.5h, 0.5h)$. Thus, the computational cells lie entirely within the squares occupied by the vortices, and the dividing streamlines lie along cell edges. The cell-averaged solution is calculated simply by averaging exact nodal-point values from a very fine grid of $h = 0.125$ unit (staggered so that points lie on the dividing streamlines and cell edges).

Figure A2 shows the two-dimensional histogram of cell-average results at $t = 3T/200$ for the six central vortices (where $\bar{\phi}$ values are nonzero). Note how the extremely sharp (nodal-point) features in the figures presented by Staniforth et al. are effectively "eroded" away when averaged over the finite-volume cells in which they occur. The "back wall," for example, which is formed from the peak of the cone being stretched along the dividing streamline at $y = 62.5$ units, is perhaps the most obvious example of this cell-average erosion.

Cell-average histograms of the type shown in Fig. A2 are the appropriate exact solutions to be used for evaluating numerical solutions for this problem. Finite-volume schemes solve for cell averages directly. Other schemes may appear to be written in terms of nodal-point values but are effectively working with cell averages. This is true, for example, for first- and second-order methods for which a nodal value is equal to its respective cell average. The nodal-point solutions presented by Staniforth et al. would only be appropriate for (third- or) higher-order methods using subcell reconstruction of the node values. For the extremely thin features of the Smolarkiewicz test problem, the exact subcell behavior is clearly rather pathological. It therefore makes much more sense to work directly in terms of cell averages.

APPENDIX B

Interpretation under Uniform Velocity Conditions

Under uniform advecting velocity conditions, the large-time-step algorithms described in this paper have an interpretation that might be described as a conservative cell-based semi-Lagrangian update. For clarity, we will first sketch the idea for COSMIC in two dimensions (the ENIGMATIC scheme has an identical analysis). Details for MACHO are different, although the result is the same. Finally, the simple-minded use of simultaneous one-dimensional fluxes is shown to be physically inconsistent. The analysis for three dimensions is entirely analogous, although obviously more complicated.

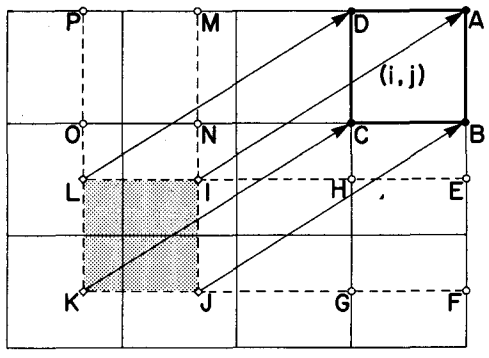

FIG. B1. Schematic diagram showing the labeling of points used in the interpretation of various algorithms under uniform velocity conditions.

a. COSMIC

Consider Fig. B1, showing various relevant points. Physically, the updated average value in cell ABCD should be the average over the shaded area IJKL. We write out the conservative flux-based algorithm to show that this, in fact, does occur. In the following, groupings in parentheses, such as (ABCD), (DCOP), etc., represent averages over the respective areas.

The two-dimensional update algorithm is

$$\bar{\phi}^+ = \bar{\phi} + c_x(\phi_w^{2D} - \phi_e^{2D}) + c_y(\phi_s^{2D} - \phi_n^{2D}). \quad \text{(B1)}$$

For COSMIC (and ENIGMATIC), in terms of averages over the indicated areas, this can be written

$$\begin{aligned}\bar{\phi}^+ = (\text{ABCD}) &+ \left\{\frac{1}{2}[(\text{DCOP}) + (\text{HGKL})] - \frac{1}{2}[(\text{ABNM}) + (\text{EFJI})]\right\} \\ &+ \left\{\frac{1}{2}[(\text{BFGC}) + (\text{NJKO})] - \frac{1}{2}[(\text{AEHD}) + (\text{MILP})]\right\}. \quad \text{(B2)}\end{aligned}$$

Expanding the area integrals involved in the various averages results in

$$\begin{aligned}\bar{\phi}^+ = (\text{ABCD}) &+ \frac{1}{2}[(\text{DCNM}) + (\text{MNOP}) + (\text{HGJI}) + (\text{IJKL})] \\ &- \frac{1}{2}[(\text{ABCD}) + (\text{DCNM}) + (\text{EFGH}) + (\text{HGJI})] \\ &+ \frac{1}{2}[(\text{BEHC}) + (\text{EFGH}) + (\text{NILO}) + (\text{IJKL})] \\ &- \frac{1}{2}[(\text{ABCD}) + (\text{BEHC}) + (\text{MNOP}) + (\text{NILO})]. \quad \text{(B3)}\end{aligned}$$

Canceling terms, we see that

$$\bar{\phi}^+ = (\text{IJKL}), \quad \text{(B4)}$$

which is correct.

b. MACHO

For (x followed by y), the MACHO scheme is

$$\bar{\phi}^+ = \bar{\phi} + c_x[\phi_w^{1D}(\bar{\phi}) - \phi_e^{1D}(\bar{\phi})] + c_y[\phi_s^{1D}(\bar{\phi}_{AX}) - \phi_n^{1D}(\bar{\phi}_{AX})]. \quad \text{(B5)}$$

In terms of averages, this is

$$\bar{\phi}^+ = (\text{ABCD}) + [(\text{DCOP}) - (\text{ABNM})] + [(\text{NJKO}) - (\text{MILP})]. \quad \text{(B6)}$$

Expanding the integrals, as before, results in

$$\bar{\phi}^+ = (\text{ABCD}) + [(\text{DCNM}) + (\text{MNOP}) - (\text{ABCD}) - (\text{DCNM})] + [(\text{NILO}) + (\text{IJKL}) - (\text{MNOP}) - (\text{NILO})]. \quad \text{(B7)}$$

Canceling terms once again gives

$$\bar{\phi}^+ = (\text{IJKL}). \quad \text{(B8)}$$

For (y followed by x), we have

$$\bar{\phi}^+ = (\text{ABCD}) + [(\text{BFGC}) - (\text{AEHD})] + [(\text{HGKL}) - (\text{EFJI})]. \quad \text{(B9)}$$

Expanding and canceling once again results in

$$\bar{\phi}^+ = (\text{IJKL}). \quad \text{(B10)}$$

c. Simultaneous one-dimensional fluxes

The simple-minded scheme based on simultaneous one-dimensional fluxes would read as follows

$$\bar{\phi}_{SM}^+ = \bar{\phi} + c_x[\phi_w^{1D}(\bar{\phi}) - \phi_e^{1D}(\bar{\phi})] + c_y[\phi_s^{1D}(\bar{\phi}) - \phi_n^{1D}(\bar{\phi})]. \quad \text{(B11)}$$

In terms of area averages, this is

$$\bar{\phi}_{SM}^+ = (\text{ABCD}) + [(\text{DCOP}) - (\text{ABNM})] + [(\text{BFGC}) - (\text{AEHD})]. \quad \text{(B12)}$$

Expanding the integrals leads to

$$\bar{\phi}_{SM}^+ = (\text{ABCD}) + [(\text{DCNM}) + (\text{MNOP}) - (\text{ABCD}) - (\text{DCNM})] + [(\text{BEHC}) + (\text{EFGH}) - (\text{ABCD}) - (\text{BEHC})]. \quad \text{(B13)}$$

This results in

$$\bar{\phi}_{SM}^+ = (\text{MNOP}) + (\text{EFGH}) - (\text{ABCD}), \quad \text{(B14)}$$

which, of course, is *not* equal to (IJKL). The update contains no information at all about the departure cell.

REFERENCES

Dukowicz, J. K., and J. D. Ramshaw, 1979: Tensor viscosity method for convection in numerical fluid dynamics. *J. Comput. Phys.*, **32,** 71–79.

Easter, R. C., 1993: Two modified versions of Bott's positive-definite numerical advection scheme. *Mon. Wea. Rev.*, **121,** 297–304.

Ekebjærg, L., and P. Justesen, 1991: An explicit scheme for advection-diffusion modelling in two dimensions. *Comp. Meth. Appl. Mech. Eng.*, **88,** 287–297.

Hólm, E. V., 1995: A fully two-dimensional, nonoscillatory advection scheme for momentum and scalar transport equations. *Mon. Wea. Rev.*, **123,** 536–551.

Hundsdorfer, W., and E. J. Spee, 1995: An efficient horizontal advection scheme for modeling of global transport of constituents. *Mon. Wea. Rev.*, **123,** 3554–3564.

Lax, P. D., and B. Wendroff, 1960: Systems of conservation laws. *Comm. Pure Appl. Math.*, **13,** 217–237.

Leith, C. E., 1965: Numerical simulation of the earth's atmosphere. *Meth. Comput. Phys.*, **4,** 1–28.

Leonard, B. P., 1991: The ULTIMATE conservative difference scheme applied to one-dimensional advection. *Comp. Meth. Appl. Mech. Eng.*, **88,** 17–74.

——, 1994: Note on the von Neumann stability of explicit one-dimensional advection schemes. *Comp. Meth. Appl. Mech. Eng.*, **118,** 29–46.

——, and M. K. MacVean, 1995: Grid-refinement study of a benchmark problem using the flux-integral method. *Quantification of Uncertainty in Computational Fluid Dynamics,* R. W. Johnson and E. D. Hughes, Eds., American Society of Mechanical Engineers, 40–50.

——, ——, and A. P. Lock, 1993: Positivity-preserving numerical schemes for multidimensional advection. NASA TM 106055, ICOMP-93-05, Lewis Research Center, Cleveland, OH, 62 pp.

——, A. P. Lock, and M. K. MacVean, 1995a: The NIRVANA scheme applied to one-dimensional advection. *Int. J. Numer. Methods Heat Fluid Flow,* **5,** 341–377.

——, M. K. MacVean, and A. P. Lock, 1995b: The flux integral method for multidimensional convection and diffusion. *Appl. Math. Modelling,* **19,** 333–342.

——, A. P. Lock, and M. K. MacVean, 1995c: Extended numerical integration for genuinely multidimensional advective transport insuring conservation. *Numerical Methods in Laminar and Turbulent Flow,* Vol. 9, C. Taylor and P. Durbetaki, Eds., Pineridge Press, 1–12.

Lin, S. J., and R. B. Rood, 1996: Multidimensional flux-form semi-Lagrangian transport schemes. *Mon. Wea. Rev.,* **124,** 2046–2070.

Rasch, P. J., 1994: Conservative shape-preserving two-dimensional transport on a spherical reduced grid. *Mon. Wea. Rev.,* **122,** 1337–1350.

Roache, P. J., 1992: A flux-based modified method of characteristics. *Int. J. Numer. Methods Fluids,* **15,** 1259–1275.

Smolarkiewicz, P. K., 1982: The multi-dimensional Crowley advection scheme. *Mon. Wea. Rev.,* **110,** 1968–1983.

——, 1984: A fully multidimensional positive definite advection transport algorithm with small implicit diffusion. *J. Comput. Phys.,* **54,** 325–362.

——, and P. J. Rasch, 1991: Monotone advection on the sphere: An Eulerian versus semi-Lagrangian approach. *J. Atmos. Sci.,* **48,** 793–810.

Staniforth, A., and J. Côté, 1991: Semi-Lagrangian integration schemes for atmospheric models—A review. *Mon. Wea. Rev.,* **119,** 2206–2223.

——, ——, and J. Pudykiewicz, 1987: Comments on "Smolarkiewicz's deformational flow." *Mon. Wea. Rev.,* **115,** 894–900.

Strang, G., 1968: On the construction and comparison of difference schemes. *SIAM J. Numer. Anal.,* **5,** 506–517.

Thuburn, J., 1996: Multidimensional flux-limited advection schemes. *J. Comput. Phys.,* **123,** 74–83.

Zalesak, S. T., 1979: Fully multidimensional flux-corrected transport algorithms for fluids. *J. Comput. Phys.,* **31,** 335–362.